JOURNAL OF CATALYSIS **177,** 259–266 (1998)
ARTICLE NO. CA982109

Critical Influence of the Amorphous Silica-to-Cristobalite Phase Transition on the Performance of $Mn/Na_2WO_4/SiO_2$ Catalysts for the Oxidative Coupling of Methane

Alejandra Palermo,* Juan Pedro Holgado Vazquez,† Adam F. Lee,‡ Mintcho S. Tikhov,‡ and Richard M. Lambert‡,[1]

*Institute of Materials Science and Technology, UNMDP-CONICET, J.B. Justo 4302, (7600) Mar del Plata, Argentina; †Instituto de Ciencia de Materiales de Sevilla, CSIC-Univ. Sevilla-Junta de Andalucía, Américo Vespucio S/N, Isla de la Cartuja, (41092), Seville, Spain; and ‡Department of Chemistry, University of Cambridge, Cambridge CB2 1EW, England

Received January 5, 1998; revised March 31, 1998; accepted April 17, 1998

XRD, XPS/XAES, TPR analysis and catalytic testing have been applied to $Na/W/Mn/SiO_2$ methane coupling catalysts and to corresponding formulations without one or more of Na, Mn, and W. We find a clear correlation between catalyst performance and support structure in the final calcined material. Amorphous silica yields active but very unselective catalysts. Crystalline SiO_2 (α-cristobalite) generates active and highly selective catalysts—especially with respect to the formation of ethylene. We demonstrate that the presence of Na is essential for the anomalous low temperature silica → cristobalite support phase transition to occur. The structural, catalytic, and spectroscopic results indicate that Na plays a dual role as both structural and chemical promoter.

Key Words: **OCM; oxidative coupling of methane; phase transition; support interaction.**

INTRODUCTION

Currently, natural gas plays only a relatively small role as a feedstock for the chemical industry, although it has long been recognised that oxidative coupling of methane (OCM) to C_2 hydrocarbons, especially ethylene, is an attractive possible route for CH_4 usage. To this end, a key technological goal is the identification of suitable catalysts capable of high ethylene selectivity at useful levels of methane conversion. Since the pioneering work of Keller and Bhasin (1), the subject has received a great deal of attention, although there is little consensus about the identity of the active surface species nor about the reaction mechanism. Keller and Bhasin tested 26 different catalyst formulations at temperatures between 773 and 1273 K; these consisted of metal oxides supported on alumina. Subsequently, a large number of oxide-based systems has been investigated, and effective OCM catalysts may be broadly classified into irreducible metal oxides, rare earth oxides, and reducible metal oxides. Additional complexities are introduced by the use of promoters, supports, and composites, and there is continuing controversy about the extent to which homogeneous gas phase chemistry contributes to the overall conversion of methane into ethane, ethylene carbon dioxide, and water. Although the very wide range of conditions used for catalyst testing by different authors makes quantitative comparisons difficult, the indications are that the most promising materials show performances on the edge of commercial usefulness. A mechanism involving gas phase coupling of surface-generated methyl radicals to yield ethane, followed by oxidative dehydrogenation of the latter to yield ethylene, seems to be generally accepted for all catalysts. There is also broad consensus that deep oxidation to yield CO_2 is a predominantly heterogeneous process. Useful reviews are to be found in references (2–8).

In part, the present work is motivated by the need to develop an active, selective, and robust system for use in a recycle-separator reactor (9) designed to produce very high selectivity at high overall conversion, thereby forming the basis for a commercially useful process.

Recently, Fang *et al.* identified (10) 1.9 wt% Mn/5 wt% Na_2WO_4/SiO_2 as a promising OCM catalyst. They proposed tetrahedral WO_4 surface species with one W=O and three W–O–Si surface bonds as the OCM active site, with manganese oxide enhancing the exchange between gaseous and lattice oxygen (11). Subsequently, this model was elaborated to include a redox mechanism involving lattice oxygen ions and the W^{+6}/W^{+5} couple (12). However, although it is true that the formation of trigrafted $(SiO)_3W{=}O$ units is plausible on, say, the (111) face of α-cristobalite, the results do not permit digrafted or monografted species to be ruled out. The same catalyst was studied by Lunsford *et al.* (13), although rather little agreement emerged as to the roles of the various chemical components in the full trimetallic working system. Moreover, the possible role of the alkali component appears to have been entirely overlooked by

[1] Corresponding author. E-mail: rml1@cam.ac.uk.

0021-9517/98 $25.00

both groups. Here, we demonstrate that the presence of Na is critically important for the genesis of an active and selective OCM catalyst. This is achieved by progressively "taking apart" the trimetallic system. In particular, it is shown that the alkali appears to play a dual role as both structural and chemical promoter and that the presence of Mn is not crucial for obtaining high ethylene yields.

METHODS

Catalyst Preparation

Trimetallic, bimetallic, and single metal formulations supported on silica were prepared and tested with the objective of pinning down the role of the individual metal components—in each case amorphous SiO_2 was the starting material for the support. The catalysts were prepared by incipient wetness impregnation of the silica support (Aldrich Davisil^{TM} 23,684-5) with aqueous solutions having appropriate concentrations of $Mn(NO_3)_2$ and Na_2WO_4. For the full trimetallic system, we used the loading employed by Lunsford *et al.*, i.e. 1.9% Mn; 5% Na_2WO_4, expressed as weight percentages. In this connection, we note that Jiang *et al.* found that methane conversion reached its limiting value at 4 wt% Na_2WO_4, further increase in Na_2WO_4 loading yielding no change in catalyst behaviour (11). It was suggested (11) that 4% loading corresponds to formation of a close-packed monolayer. Alkali-free materials were synthesised by using $(NH_4)_2WO_4$ as a precursor, Mn- and W-free samples being prepared by impregnation of silica with the alkali hydroxide. The catalysts were then dried for 6–8 h at 120°C and calcined in flowing oxygen for 8 h at 850°C, except where noted. The $(NH_4)_2WO_4$ + Na/SiO_2 sample was prepared by using as a support the Na/SiO_2 control sample, already calcined at 850°C, and thus already transformed to α-cristobalite. This material was then impregnated with an aqueous solution of $(NH_4)_2WO_4$. The amounts of the various metal components in the different samples were always the same as the full trimetallic catalyst (1.9% Mn; 5% Na_2WO_4).

For use in control experiments, highly crystalline synthetic α-cristobalite was prepared by heating pure amorphous silica to 1600°C for 50 h. A control sample (Na/SiO_2) was also prepared by adding dissolved Na(OH) to the amorphous silica, so that the total amount of Na was the same as that in the Na_2WO_4/SiO_2 and $Mn/Na_2WO_4/SiO_2$ samples. This latter sample was dried and calcined as described above. The specific surface area of the samples was measured by the BET method in a volumetric system at liquid nitrogen temperature with N_2 as adsorbate.

XRD Analysis

X-ray diffraction patterns of the fresh and used catalysts were obtained with a Philips PW 1710 diffractometer using CuK_α radiation. Diffractograms were recorded from $2\theta =$ 10–70° with the detector moving in $\Delta 2\theta = 0.05°$ steps to achieve good angular resolution.

TPR Measurements

A conventional temperature-programmed reduction apparatus was used with the reactive gas stream (10% H_2 in Ar, 99.996%, 50 ml min^{-1}) being passed through the reference branch of the katharometer, then through the quartz reactor containing 0.1 g of sample. Each run was conducted between room temperature and 950°C at a constant heating rate of 10°C min^{-1} (Eurotherm 2416).

Microreactor Testing

Measurements were carried out using a single-pass, plug-flow microreactor, equipped with on-line gas chromatographic sampling (GCPerkin Elmer HWD Sigma 300 and Perkin Elmer LCI-100 Integrator) analysis using a 60–80 Carboxen-1000 column. The reactor consisted of a down flow alumina tube (DEGUSSIT AL23 $6 \times 3 \times 400$ mm) with 0.4 g of catalyst and alumina wool above and below the catalyst bed to retain the sample. Blank runs with the alumina tube and alumina wool and without catalyst showed negligible reaction up to 900°C. A K-type thermocouple was attached to the outside wall of the reactor. Reactant gases (20% CH_4 in He (99.95%) and 20% O_2 in He (99.996%)) were used without further purification. Gas flowrates were regulated by mass flow controllers (Brooks 5890). Testing was carried out at 850°C and 2000 h^{-1} space velocity with reactant composition methane: oxygen 4.5 to 1 at a total pressure of 1 atm. These experimental conditions produced optimal performance with Mn/Na_2WO_4/silica catalyst and were used for all samples as the fixed basis for comparison. At the reactor outlet an ice trap was used to remove the water in the product gases when a catalyst was kept on stream for several hours. Before admission of the reactant mixture, each catalyst sample was heated in flowing oxygen at 10°C min^{-1} up to reaction temperature.

XPS Measurements

XPS data were acquired in a VG ADES 400 UHV spectrometer system. Catalyst samples were mounted using a method free from organic contamination by pressing a small amount of the material between two discs of pure aluminium. Separating the latter then gave two specimens consisting of a thin film of catalyst powder cohering to the Al. XP spectra were acquired with $MgK\alpha$ radiation. Quoted binding energies (BEs) are referred to the Si 2p emission at 103.5 eV, unless otherwise stated.

RESULTS AND DISCUSSION

XRD Analysis

Representative samples of fresh and used catalysts containing one, two, and three metallic components were examined by X-ray diffraction. The precursor silica support was amorphous (Fig. 1a) and Fig. 1d shows the XRD pattern obtained after 750°C calcination of the 1.9% Mn/5% Na_2WO_4/SiO_2 catalyst precursor: reflections assigned to Na_2WO_4, Mn_2O_3, and α-cristobalite are clearly apparent. Thus the initially amorphous silica underwent complete conversion to highly crystalline α-cristobalite during calcination at a temperature far below the normal transition temperature of 1500°C. (For comparison purposes, the XRD pattern of our synthetic α-cristobalite is shown in Fig. 1b.) The same anomalous low temperature SiO_2 phase transition resulted upon calcining Na_2WO_4 supported on amorphous silica (Fig. 1c). Although this remarkable phase transition has been noted before (10, 12), its possible catalytic significance appears to have been overlooked.

In order to determine which of the three metallic components is responsible for the dramatic change in SiO_2 structure, samples containing only Mn, W, or Na were prepared and calcined at different temperatures ranging from 750 to 900°C. As can be seen from Figs. 2a and 2b, neither Mn nor W alone induce the low temperature phase transition. Figure 3 shows that Na is the crucial component for inducing crystallisation. Thus, although Na(OH) on silica calcined at 750°C yields an amorphous product, raising the temperature to 900°C leads to complete crystallisation with the formation of α-cristobalite and the closely related phase α-tridymite. This result, taken with those illustrated in Figs. 1b and 1c, shows that while Na is necessary and sufficient for the low temperature phase transition, the presence of W renders the Na even more effective. We may infer that there is a strong interaction between Na and the silica support and that this is enhanced by the W. As will be apparent from the results which follow, the final structure of the SiO_2 and the extent of its chemical interaction with Na are both critically important in determining whether or not an active and selective catalyst is produced.

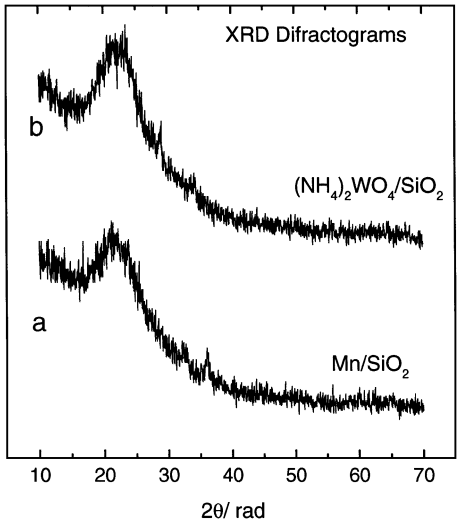

FIG. 2. XRD spectra of various samples after calcination at 900°C: (a) Mn/SiO_2; (b) $(NH_4)_2WO_4/SiO_2$.

Microreactor Results

Catalytic testing was performed on samples of (i) amorphous silica, (ii) $Mn/Na_2WO_4/SiO_2$, (iii) Na_2WO_4/SiO_2, (iv) $(NH_4)_2WO_4/SiO_2$, (v) Mn oxide supported on silica,

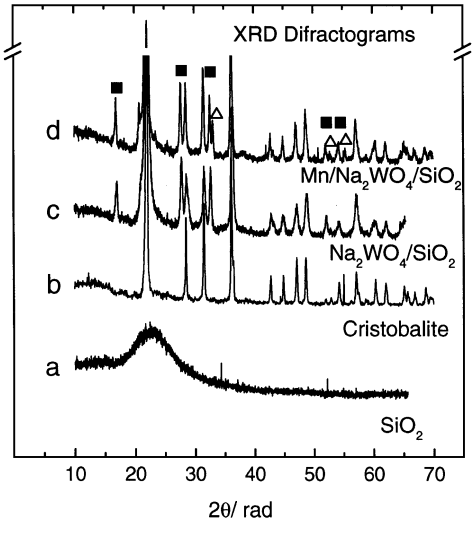

FIG. 1. XRD spectra of various samples after calcination at 750°C: (a) SiO_2; (b) $Mn/Na_2WO_4/SiO_2$; (c) Na_2WO_4/SiO_2; (d) α-cristobalite. (■) Na_2WO_4; (Δ) Mn_2O_3.

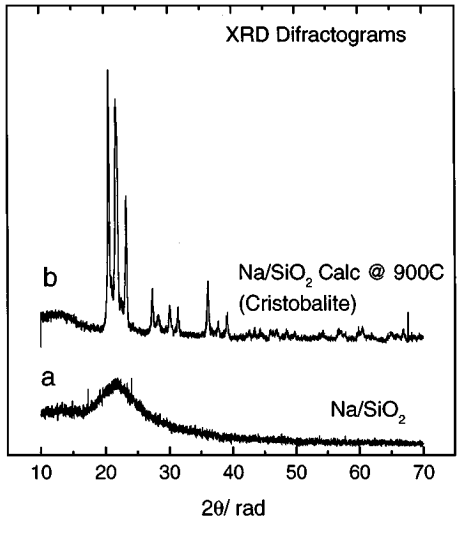

FIG. 3. XRD spectra of Na(OH) supported on amorphous silica at different samples: (a) Na/SiO_2 after calcination at 750°C; (b) Na/SiO_2 after calcination at 900°C.

TABLE 1

Crystalline Structure and Catalytic Activity/Selectivity Behaviour of Different Samples for Oxidative Coupling of Methane[a]

Catalyst	Structure	Surface area ($m^2\ g^{-1}$)	CH_4 conversion (%)	Total C_2's selectivity (mol %)	C_2H_4 selectivity (mol %)	$\eta_{C_2H_4}$ yield
$Mn/Na_2WO_4/SiO_2$	α-Cristobalite	4	33	80	>50	>17
Na_2WO_4/SiO_2	α-Cristobalite	3	44	52	42	18.5
$Mn/(NH_4)_2WO_4/SiO_2$	Amorphous	135	20	40	30	6
Mn/SiO_2	Amorphous	130	23	23	19	4.3
$(NH_4)_2WO_4/SiO_2$	Amorphous	135	12	20	15	1.8

[a] $T = 850°C$; $CH_4 : O_2 = 4.5 : 1$; total flow rate = 18 cc/min; 0.4 g catalyst.

(vi) NaOH supported on silica (and treated at different calcination temperatures), and (vii) NaOH supported on synthetic α-cristobalite. The extent of methane conversion (X_{CH_4}), selectivity to ethane plus ethylene (S_{C_2}), ethylene selectivity ($S_{C_2H_4}$), and the ethylene yield ($\eta_{C_2H_4}$: moles of ethylene produced per mol of methane consumed) are presented in Table 1 for the optimum operating conditions of 850°C, $CH_4 : O_2 = 4.5 : 1$ for 0.4 g of $Mn/Na_2WO_4/SiO_2$ at a space velocity of 2000 h^{-1}. (We explored temperatures from 700 to 950°C and $CH_4 : O_2$ from 2 : 1 to 12 : 1, all at GHSV 2000 h^{-1}.)

In agreement with the earlier workers, we find that the full trimetallic formulation $Mn/Na_2WO_4/SiO_2$ calcined at 750°C generates an excellent catalyst in terms of high C_2 selectivity (80%) at high conversion (33%) under the standard test conditions described above (row 1, Table 1). Note that the *ethylene* selectivity is particularly good (>50%)—this is a most important characteristic in regard to technical implementation and was not reported by the earlier workers (10–12). Eliminating only the Mn component (row 2, Table 1) leaves the overall activity nearly unchanged, but significantly decreases the total C_2 selectivity, in agreement with Wu and Li (14); however, the ethylene selectivity is much less affected (42%). Note that in this case the support does undergo conversion to α-cristobalite and we still have a "good" catalyst. Eliminating only the Na component (row 3, Table 1) immediately produces a bad, unselective catalyst in which the support phase consists of amorphous silica. Eliminating both Na and W (row 4, Table 1) produces an even worse catalyst. By comparison with rows 1 and 3, one may conclude that there is strong synergy only when the three metal components are present simultaneously, a situation that also leads to Na-induced crystallisation of the support.

For present purposes, a comparison between rows 5 and 2 is the most interesting. Na tungstate generates a "good" catalyst supported on α-cristobalite; ammonium tungstate produces a bad catalyst supported on amorphous silica—both activity and selectivity are low. In fact, ammonium tungstate on amorphous silica yields a catalyst that is no better than amorphous silica itself (compare with row 1, Table 2). We conclude that Na plays the role of a structural promoter, converting amorphous silica (which acts mainly to burn methane and hydrocarbon products) into α-cristobalite—which is effectively inert under reaction conditions (see below).

Table 2 summarises the results of additional experiments that were designed to focus further on the role of Na and on the catalytic significance of the amorphous → crystalline

TABLE 2

Crystalline Structure and Catalytic Activity/Selectivity Behaviour of Different Samples for Oxidative Coupling of Methane[a]

Catalyst	Structure	Surface area ($m^2\ g^{-1}$)	CH_4 conversion (%)	Total C_2's selectivity (mol %)	C_2H_4 selectivity (mol %)	$\eta_{C_2H_4}$ yield
SiO_2	Amorphous	150	17	~23	~15	~2
Na/SiO_2	Amorphous	130	13	~15	n.d.	n.d.
Na/SiO_2 (900°C)	α-Cristobalite	5	<2			
Na_2WO_4/α-cristobalite	α-Cristobalite	2	8	54	20	2
$(NH_4)_2WO_4$/α-cristobalite	α-Cristobalite	2	<5	<5	0	0
$Na/SiO_2 + (NH_4)_2WO_4$	α-Cristobalite	6	9	53	20	2

[a] $T = 850°C$; $CH_4 : O_2 = 4.5 : 1$; total flow rate = 18 cc/min; 0.4 g catalyst.

phase transition in the SiO_2 carrier. As already mentioned, amorphous silica itself behaves as a very unselective catalyst under these conditions (row 1). Loading with NaOH (same Na mol% as in the original formulation) and calcining at 750°C yields an amorphous material which is also a poor, unselective catalyst (row 2). However, calcining the same precursor to 900°C yields Na/α-cristobalite *and this material is effectively inert* (row 3). This strongly supports our proposal above, namely that one role of Na is that of a structural promoter which converts the active and unselective amorphous silica carrier into a catalytically inert crystalline phase.

The remaining results in Table 2 were acquired in order to examine (i) whether or not the presence of Na *during* the transformation to α-cristobalite is significant, and (ii) whether Na plays an additional role as a "chemical" promoter. To this end, samples were prepared using pure synthetic α-cristobalite as the starting material for the carrier phase. A comparison of row 4, Table 2 with row 2, Table 1 is revealing. In both cases the final material corresponds to Na_2WO_4 on α-cristobalite. However, *when the α-cristobalite is produced during catalyst genesis* the resulting material is clearly superior in terms of both activity and selectivity. It is possible that this is related to an improved dispersion, or even chemical bonding, of the Na on the α-cristobalite surface when the latter is generated *in situ*. The XPS/XAES data (see below) shed some light on this issue. When $(NH_4)_2WO_4$ replaces Na_2WO_4 as the precursor on synthetic α-cristobalite, one obtains an inactive and unselective catalyst (compare rows 4 and 5 of Table 2). This interesting observation suggests that Na also plays a role as a chemical promoter, stabilising the W component in the appropriate state. Based on Raman data, Wang *et al.* (13) concluded that a surface bound distorted WO_4 tetrahedron was the OCM active site. In the Na-free case, it is reasonable to suppose that a different form of W(VI) is produced at the surface, perhaps a material akin to WO_3 in which the W atoms are octahedrally co-ordinated.

As a control experiment, we tested pure unsupported Na_2WO_4 in order to determine whether its presence, when detectable by XRD, has a significant influence on catalyst performance. Catalysts **c** and **d** in Fig. 1 are examples of this. Under the conditions specified in Table 2 we found 8% methane conversion with total C_2 and ethylene selectivities of 46 and 27% respectively—i.e., similar to Na_2WO_4/α-cristobalite (row 3, Table 2). That is, crystalline Na_2WO_4 is an ineffectual OCM catalyst. This is consistent with the results of Jiang *et al.* (11) which show that on silica Na_2WO_4 loadings in excess of 4 wt% (we used 5%) lead to no changes in catalyst performance, implying that the excess Na_2WO_4 is present as crystallites which do not contribute measurably to catalyst performance.

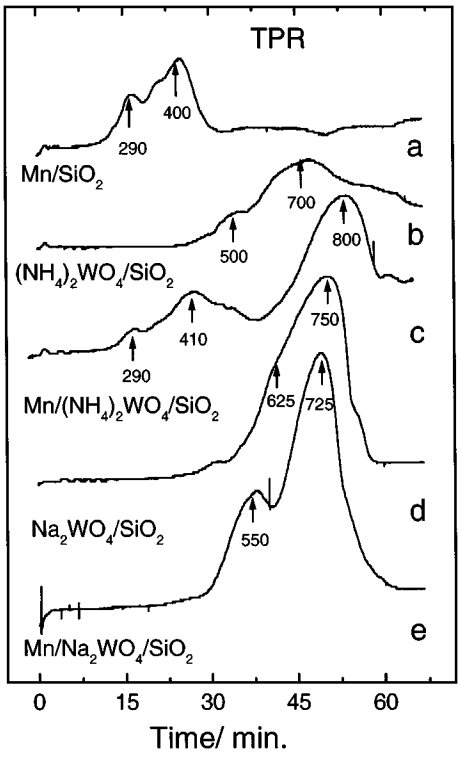

FIG. 4. Temperature programmed reduction (TPR) profiles for: (a) Mn/SiO_2; (b) $(NH_4)_2WO_4/SiO_2$; (c) $Mn/(NH_4)_2WO_4/SiO_2$; (d) Na_2WO_4/SiO_2; (e) $Mn/Na_2WO_4/SiO_2$.

Temperature Programmed Reduction

Figure 4 shows data obtained with fresh calcined samples containing one (Mn, W), two (Mn + W), (Na + W), and three (Mn + Na + W) metal components. Trace **a** shows a broad feature with peaks at 290 and 400°C which we associate with Mn; similarly, the broad feature in **b** is associated with W. The addition of Mn to W (trace **c**) upshifts mainly the characteristic reduction features of W. Na added to W has a similar effect to Mn in upshifting the W reduction peak (trace **d**). This suggests that there is significant interaction between the Mn and W components, *and* between Na and W. The latter is consistent with our proposal based on the reactor results that there is a strong interaction between Na and WO_4 entities. It is also in line with the XRD results which indicate a co-operative effect between Na and W in the crystallisation of silica. The trimetallic system (trace **e**) shows a peak at 550°C which we tentatively associate with reduction of a perturbed Mn species, given the intensity of the Mn features in the control sample (trace **a**). This is not an unambiguous assignment, given the proximity of the 625 and 500°C peaks found for the Na/W and W-only formulations (traces **d** and **b**, respectively). However, the data do suggest strong interaction between all the metal components in the full trimetallic formulation; this is consistent with the reactor data which suggest that

there is particularly strong synergy when all three metals are present.

X-Ray Photoelectron Spectroscopy

A detailed survey of the various catalyst samples and appropriate control samples was carried out by XPS/XAES. Observations were made on the Si 2p, O 1s, W 4f, Na 1s core levels, and on the Na KLL Auger emission for samples prepared from the following precursors:

a	$(NH_4)_2WO_4/SiO_2$	→ bad catalyst; *active*, *unselective*
b	Na_2WO_4/SiO_2	→ good catalyst; *active*, *selective*
b2	$(NH_4)_2WO_4 + Na/SiO_2$	→ fair catalyst; *low activity*, *selective*
c	Na_2WO_4/α-cristobalite	→ fair catalyst; *low activity*, *selective*
d	Na_2WO_4	→ reference compound
e	Na/SiO_2	→ inert catalyst.

The measured BE differences between Si 2p and W 4f were identical for all the SiO_2-supported materials, suggesting that differential charging effects were not serious between these cases. Of course, no such direct comparison is available for the bulk Na_2WO_4 control sample which contains no SiO_2. In order to permit approximate BE comparisons between this material and the SiO_2 supported materials, we proceeded as follows. For the SiO_2-containing samples, the Si 2p emission was used for calibration (103.5 eV). No striking differences emerge between the various O 1s, O 2s, and Si 2p spectra, as might be expected in view of the limited resolution due to use of unmonochromated radiation and the large amount of SiO_2 present in the support phase. For the reference compound, Na_2WO_4 , the O 1s emission was used for calibration, assigning it the same binding energy as in the other samples. This provides a coherent BE scale, with the W 4f BE then occurring at the value expected for W^{6+} and similar to the W 4f BE found in the SiO_2-containing samples.

From Fig. 5 it can be seen that the O 2s emission intensities are very similar for sample **b** (good catalyst) compared to sample **a** (bad catalyst). Comparison with the O 2s emission from pure Na_2WO_4 and from Na/SiO_2 (not shown) demonstrates that *the O 2s emission in the Fig. 5 spectra is almost entirely due to oxygen in the silica rather than oxygen associated with WO4*. This is consistent with well dispersed W species on **b** and poorly dispersed W species on **a**. We note in passing that, although the XRD data for the "good" catalyst shows crystalline Na_2WO_4, the reactor control experiment with pure Na_2WO_4 shows that the latter is catalytically ineffectual. Therefore, the above reasoning about the nature of the "good" catalyst is unaffected by the presence in this catalyst of XRD-visible Na_2WO_4.

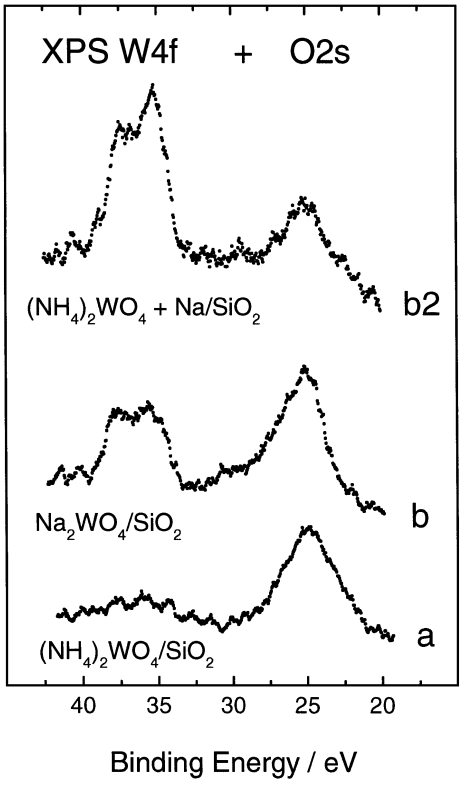

FIG. 5. O 2s and W 4f XPS for: (a) $(NH_4)_2WO_4/SiO_2$; (b) Na_2WO_4/SiO_2; (c) $(NH_4)_2WO_4/SiO_2 + Na/SiO_2$.

As shown above, Na plays a critical role in causing the amorphous silica → α-cristobalite phase transition. The data shown for sample **c** were recorded in order to try and establish whether the Na does indeed play a dual role, as suggested by the reactor results. Sample **b2** was prepared by (i) calcining amorphous silica impregnated with the appropriate amount of NaOH; this induced the silica → α-cristobalite transition and then (ii) impregnating with the appropriate amount of $(NH_4)_2WO_4$ and re-calcining; i.e. the WO_4 was introduced by the same Na-free route as that employed with sample **a**. It is apparent that the ratio of the W 4f/O 2s intensities is similar to that found for sample **b**, the good catalyst. Interestingly, sample **c** is a selective and quite active catalyst. Together, these spectra imply that Na on the SiO_2 surface is necessary for obtaining good dispersion of the WO_x species, thought to be the catalytically active agent.

Figure 6 shows the Na 1s XP spectra obtained from samples **a**–**e**. Spectrum **a** confirms that the bad catalyst obtained from the $(NH_4)_2WO_4/SiO_2$ precursor does indeed have a sodium-free surface. The ~1075 eV BE implies a photoelectron kinetic energy of ~175 eV; i.e., these spectra are quite "surface sensitive." Comparison of spectra **b** (good catalyst) and **e** (inert catalyst) indicate that the Na is in a similar chemical state in these two samples. Both materials have undergone conversion to α-cristobalite, and the

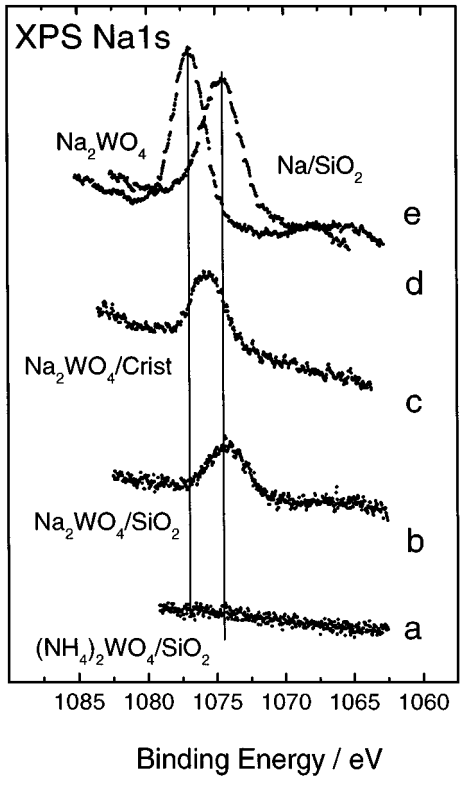

FIG. 6. Na 1s XPS for: (a) $(NH_4)_2WO_4/SiO_2$; (b) Na_2WO_4/SiO_2; (c) Na_2WO_4/α-cristobalite; (d) Na/SiO_2 (after calcination at 900°C); (e) Na_2WO_4.

dramatic lowering of the transition temperature strongly suggests that in both cases the Na is incorporated in the SiO_2 structure (15). Spectrum **d** is a reference spectrum obtained from bulk Na_2WO_4. Comparison with spectrum **c** (selective, quite active catalyst, *made by starting with α-cristobalite*) shows that the Na 1s emission from the latter is intermediate between that from the bulk tungstate (**d**) and that from the "SiO_2-bound" Na in the *in situ* crystallised α-cristobalite (**b**, **e**).

The Na KLL XAES spectra (Fig. 7) complement the Na 1s XP spectra, because the associated sampling depth is significantly greater (electron kinetic energy ~987 eV; $\lambda \sim 10$ layers). Detailed analysis of these spectra in terms of Na electronic structure is not possible because there have been no systematic studies of the Na KLL lineshape and emission energy. However, they do serve to distinguish different Na environments. Spectrum **a** confirms the absence of Na in the near surface region of the sodium-free sample. Comparison of spectrum **b** (active, selective catalyst) with spectra **d** and **e** indicates that the Na in the "good" catalyst is distinct from Na associated with WO_4 alone, Na associated with silica alone, and Na in the inactive although quite selective catalyst **c**. Spectrum **b** could therefore correspond to Na associated with both silica and WO_4—i.e., it forms part of the catalytically active phase.

The fact that Na_2WO_4/SiO_2 (initially amorphous) upon calcination yields a much better catalyst than Na_2WO_4/SiO_2 (initially α-cristobalite) shows that something must be present in the former which is missing in the latter. This is further evidence that the "good" catalyst does indeed contain well-dispersed WO_4.

A plausible view of the bimetallic catalyst could thus be as follows. Na-mediated conversion of the amorphous silica support phase to α-cristobalite is of key importance in converting an otherwise deleterious carrier to a truly inert material covered by a near monolayer of OCM active species. Notice that, although amorphous silica is itself an undesirable component in the final material, its presence in the precursor is essential for production of an active selective catalyst; it plays a positive role in helping to build the active sites. This method of catalyst synthesis also serves to disperse and bond the Na to the α-cristobalite surface in a particularly effective way, suggesting that the principal catalytically active species consists of adsorbed WO_x bonded to the SiO_2 network in the presence of Na.

In our discussion we have tended to neglect the role of the Mn component, about which in any case there is disagreement in the literature. This is so because our principal objective was to uncover the role of Na, the species which clearly causes the silica crystallisation and which appears

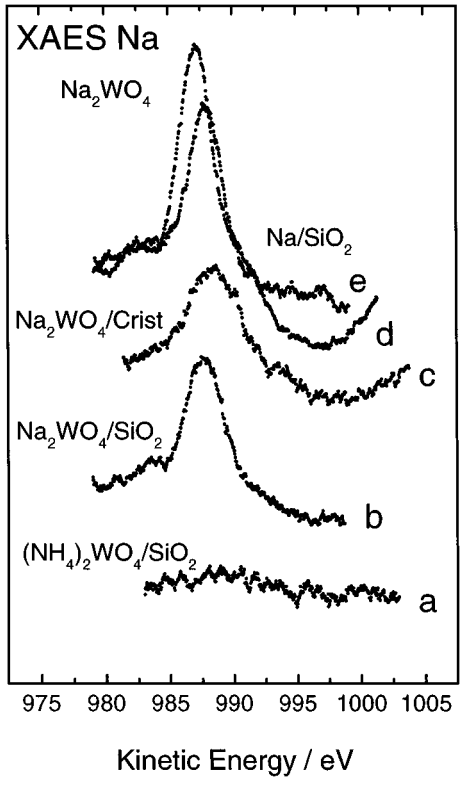

FIG. 7. Na KLL XAES: (a) $(NH_4)_2WO_4/SiO_2$; (b) Na_2WO_4/SiO_2; (c) Na_2WO_4/α-cristobalite; (d) Na/SiO_2 (after calcination at 900°C); (e) Na_2WO_4.

to be associated with the W component; the Mn does not cause the silica to crystallise. Our current work is aimed at elucidating the role of Mn in this interesting although complex catalyst. In this connection, we note that Jones *et al.* (16) showed that the performance of silica/manganese oxide OCM catalysts can be increased by the addition of alkali metals and alkaline earths. They obtained the highest C_2 selectivity with sodium as a promoter and argued that the effect of Na is to increase surface basicity, decrease surface area, and convert nonselective manganese oxide into a more selective form. However, the possibility of Na-induced crystallisation of the support was overlooked.

CONCLUSIONS

1. During OCM catalyst precursor calcination, it is the presence of Na which induces crystallisation of the amorphous silica carrier at temperatures far below the normal transition temperature. This effect of Na is enhanced by the simultaneous presence of W, resulting in the formation of highly crystalline α-cristobalite at only 750°C.

2. The good activity and very high C_2 selectivity at high methane conversion of the full trimetallic Mn, Na, W formulation on α-cristobalite is confirmed. Additionally, very good selectivity towards ethylene is found.

3. Reactor data, XRD, Na 1s XP, W 4f, and Na KLL Auger spectra indicate that Na plays a dual role as both structural and chemical promoter. First, it induces conversion of the (methane-burning) amorphous silica support to catalytically inert α-cristobalite. Second, it acts to disperse and stabilise the key W surface species, possibly WO_4, thought to be implicated as the OCM active site.

4. When α-cristobalite is produced from amorphous silica during catalyst genesis, the resulting material is more effective than when pure α-cristobalite is used as starting material. It seems possible that in the former case improved anchoring and/or dispersion of the WO_4-stabilising Na component occurs.

ACKNOWLEDGMENTS

Support under the Joule-Thermie III programme of the European Community is gratefully acknowledged (Grant JOE3CT950010). This work was also partly supported under UK EPSERC Grant GRK/45562. A.P. thanks CONICET, Argentina for financial support; J.P.H.V. thanks The Spanish Ministerio de Educación and the European Commission for financial support. We are indebted to Dr. Martin Dove, Cambridge University Department of Earth Sciences, for preparing the sample of synthetic α-cristobalite.

REFERENCES

1. Keller, G. E., and Bhasin, M. M., *J. Catal.* **73**, 9 (1982).
2. Lee, J. S., and Oyama, S. T., *Catal. Rev.-Sci. Eng.* **30**(2), 249 (1988).
3. Anderson, J. R., *Appl. Catal.* **47**, 177 (1989).
4. Amenomiya, Y., Birss, V. I., Goledzinowski, M., Galuszka, J., and Sanger, A. R., *Catal. Rev.-Sci. Eng.* **32**(3), 163 (1990).
5. Lunsford, J. H., *Catal. Today* **6**, 235 (1990).
6. Zhang, Z., Verykios, X. E., and Baerns, M., *Catal. Rev.-Sci. Eng.* **36**(3), 507 (1994).
7. Voskresenskaya, E., Roguleva, V. G., and Anshits, A. G., *Catal. Rev.-Sci. Eng.* **37**(1), 101 (1995).
8. Qiu, X., Wong, N., Tin, K., and Zhu, Q., *J. Chem. Tech. Biotechnol.* **65**, 303 (1993).
9. Jiang, Y., Yentekakis, I. V., and Vayenas, C. G., *Science* **264**, 1563 (1994).
10. Fang, X. P., Li, S. B., Lin, J. Z., Gu, J. F., and Yang, D. X., *J. Mol. Catal. (China)* **6**, 427 (1992).
11. Jiang, Z.-C., Yu, C.-J., Fang, X.-P., Li, S. B., and Wang, H.-L., *J. Phys. Chem.* **97**, 12870 (1993).
12. Wu, J., Li, S., Niu, J., and Fang, X., *Appl. Catal. A: General* **124**, 9 (1995).
13. Wang, D., Rosynek, M. P., and Lunsford, J. H., *J. Catal.* **155**, 390 (1995).
14. Wu, J., and Li, S., *J. Phys. Chem.* **99**, 4566 (1995).
15. Wells, P. B., "Structural Inorganic Chemistry," Chap. 23, p. 1004. Oxford Univ. Press, Oxford, 1987.
16. Jones, C. A., Leonard, J. J., and Sofranko, J. A., *J. Catal.* **103**, 311 (1987).